

Effective potential of a black hole in thermal equilibrium with quantum fields

David Hochberg* and Thomas W. Kephart†

Department of Physics and Astronomy, Vanderbilt University, Nashville, Tennessee 37235

James W. York, Jr.‡

*Institute of Field Physics and Theoretical Astrophysics and Relativity Group, Department of Physics and Astronomy
University of North Carolina, Chapel Hill, North Carolina 27599-3255*

(Received 2 August 1993)

Expectation values of one-loop renormalized thermal equilibrium stress-energy tensors of free conformal scalars, spin- $\frac{1}{2}$ fermions, and U(1) gauge fields on a Schwarzschild black hole background are used as sources in the semiclassical Einstein equation. The back reaction and new equilibrium metric have been found at $O(\hbar)$ for each spin field in previous work. In this paper, the nature of the modified black hole spacetime is explored through calculations of the effective potential for null and timelike orbits. Significant novel features affecting the motions of both massive and massless test particles show up at lowest order in $\epsilon = (M_{\text{Pl}}/M)^2 < 1$, where M is the black hole mass, and M_{Pl} is the Planck mass. Specifically, we find an increase in the black hole capture cross sections, and the existence of a region near the black hole with a repulsive contribution, generated by the U(1) back reaction, to the gravitational force. There is no such effect for other spins. Extrapolating our results suggests a tendency towards the formation of stable circular orbits, but the result cannot be established in $O(\hbar)$: the change in the metric becomes large and it changes its signature. We also consider the back reaction arising from multiple fields, which ultimately should be useful for treating a black hole in equilibrium with field ensembles belonging to gauge theories. In certain circumstances, however, reliable results will require calculations beyond $O(\hbar)$.

PACS number(s): 04.70.Dy, 04.20.Cv, 97.60.Lf

I. INTRODUCTION

A black hole can exist in thermodynamical equilibrium provided it is surrounded by radiation with a suitable distribution of stress energy. Appropriate heat baths are composed of quantum fields interacting with the black hole geometry. The gravitational effect of the heat bath is characterized by its gravitationally induced renormalized stress-energy tensor. One can use the expectation value of stress-energy tensors of quantum fields renormalized over the classical spacetime geometry of a black hole as the source in the semiclassical Einstein equation,

$$G_{\nu}^{\mu} = 8\pi \langle T_{\nu}^{\mu} \rangle_{\text{renormalized}}, \quad (1)$$

to calculate the change induced by the stress-energy tensor on the black hole's spacetime metric. This is the back-reaction problem associated with the spacetime geometry of a black hole in thermal equilibrium.

In this paper we use the solutions of the back reaction equation (1) given in [1] to investigate in detail the modifications to the Schwarzschild geometry arising from the interaction between the black hole and various types of quantum fields. For source terms we take the one-loop

quantum stress-energy tensors computed for conformal scalars, massless spin- $\frac{1}{2}$ fermions, and U(1) gauge bosons. The nature of the modified spacetime geometry is revealed through the effective potential, which completely characterizes the motion of test particles moving in the modified background. We calculate the effective potential for both massless and massive test particles and separate out the back-reaction contributions coming from each spin type $(0, \frac{1}{2}, 1)$, because, as it turns out, there are important qualitative distinctions among the various spins. Moreover, we will ultimately want to be able to discuss the back reactions arising from particular weighted sums of the separate spin-dependent cases in order to be able to address the problem of black holes in equilibrium with a thermal ensemble containing the field content of gauge theories of particle physics.

From the properties of the renormalized stress-energy tensors we employ and of the semiclassical Einstein equation, we have obtained in [1] accurate fractional corrections to the metric in $O(\epsilon)$, where $\epsilon = \hbar M^{-2}$, $M_{\text{Pl}} = \hbar^{1/2}$ is the Planck mass and M is the mass of the black hole (units are chosen such that $G = c = k_B = 1$, but $\hbar \neq 1$). This means we will be restricted to considering the $O(\epsilon)$ corrections to the effective potential. The effects we study will be at most of qualitative significance for small (hot) black holes, such as might have existed in the early Universe. Yet, already at this lowest order, suggestive trends are evident in the effective potential. Indeed, as we will see, there is a general trend (for each spin case)

*Electronic address: hochbed@vuctrvax

†Electronic address: kephartt@vuctrvax

‡Electronic address: york@physics.unc.edu

for the overall magnitude of the potential to decrease as the strength of the back reaction is increased, that is, as $\epsilon \rightarrow 1$ or as the number of fields increases. For the cases we have considered, the potentials all turn over at about $\epsilon \approx 0.5$ and tend toward local minima, but then one is leaving the domain of validity of the calculation and the existence of local minima is not unambiguously determined. Higher-order (or nonperturbative) calculations are required to settle this issue. For timelike geodesics, the back reaction leads to the formation of stable circular orbits even when the test particles have an angular momentum *less* than the critical value associated with stable orbits for the classical Schwarzschild black hole.

Another important feature which shows up at $O(\epsilon)$ is a consequence of the gauge boson back reaction. For this case, and this case only, we find the back reaction generates a repulsive *antigravity* contribution to the net force in the region surrounding the renormalized black hole event horizon. This repulsive component of the effective potential should not be confused with the ordinary repulsive angular-momentum-dependent barrier term which arises in all central force problems, nor should it be confused with the reversal in sign of the centripetal acceleration for a circular orbit inside $r=3M$ for an ordinary Schwarzschild hole [2]. Indeed, the existence of this new repulsive force is confirmed by an explicit calculation of the acceleration of a test particle initially at rest (hence, with zero angular momentum). In the absence of any back reaction, the radial acceleration is proportional to $-\hat{r}$, where \hat{r} is the outward unit radial vector. With the back reaction, we find the $O(\epsilon)$ correction to the acceleration is proportional to $+\hat{r}$, from roughly $r \approx 2.8M$ out to $r \approx 8.6M$, indicating the presence of an outwardly directed force. This holds for a single gauge boson and for all $\epsilon > 0$.

The features mentioned so far reflect the physics of the back reaction of a single species ($N=1$) of each field of a given spin. It is also interesting to consider the effect of the back reaction due to multiple fields ($N > 1$) of a given spin. This, in fact, is the situation one expects to encounter when the black hole interacts with a thermal ensemble of fields belonging to multiplets (representations) of specific gauge groups which arise in modern theories of particle physics. The effective potentials for multiple species are constructed simply by scaling the $N=1$ potential correction terms with numerical coefficients which count the number, or multiplicity, of fields of a given spin that occur in the particular gauge group. We will work in the lowest approximation where all matter and gauge fields are free. One obvious consequence of this multiple field back reaction is that the effects mentioned above occur for smaller values of the perturbation parameter ϵ than for the $N=1$ cases. However, the corresponding domain of validity of our perturbative calculations decreases with increasing particle multiplicity, and this point must be accounted for carefully. Unfortunately, we cannot fully achieve the multiplicities required in all cases of interest without going beyond $O(\hbar)$. For the U(1) case, the presence of the repulsive “core” and its effects become pronounced as the number of gauge bosons interacting with the black hole increases.

II. STRESS-ENERGY TENSORS AND SOLUTION OF THE BACK REACTION

Exact one-loop stress-energy tensors renormalized on a Schwarzschild background have been computed for conformal scalar fields and for U(1) gauge bosons, respectively, by Howard, Howard, and Candelas [3] and by Jensen and Ottewill [4]. Both these results can be expressed in the form

$$\langle T_{\nu}^{\mu} \rangle_{\text{renormalized}} = \langle T_{\nu}^{\mu} \rangle_{\text{analytic}} + \left[\frac{\hbar}{\pi^2(4M)^4} \right] \Delta_{\nu}^{\mu}, \quad (2)$$

where the analytic piece, in the case of the conformal scalar field, was first given by Page [5]. The term Δ_{ν}^{μ} is obtained from a numerical mode sum. As this term is small in comparison to the analytic piece, we do not include it in the calculations in this paper. This does not affect any of our qualitative results or methods because both pieces separately obey the required regularity and consistency conditions. Moreover, the analytic piece has the correct trace anomaly in both cases. An analytic approximation for the stress-energy tensor of a massless spin- $\frac{1}{2}$ fermion has been computed by Brown, Ottewill, and Page [6]. As far as we are aware, its accuracy has not been verified by an exact numerical analysis, unlike the scalar and vector cases.

Each of the above mentioned tensors has the asymptotic form of a flat spacetime radiation stress-energy tensor at the uncorrected Hawking temperature (T_H) at infinity of an ordinary Schwarzschild black hole:

$$T_{\nu}^{\mu} \rightarrow \text{const} \times \text{diag}(-3, 1, 1, 1)_{\nu}^{\mu}. \quad (3)$$

In what follows, it is convenient to write the radial and lateral pressures of the U(1) radiation at infinity as (no sum on i)

$$(T_i^i)_{\infty} \equiv \frac{1}{3} a T_H^4 = \frac{\epsilon}{48\pi K M^2}, \quad (4)$$

where $K=3840\pi$, $a=(\pi^2/15\hbar^3)$, $T_H=\hbar/8\pi M$ is the Hawking temperature at infinity, and $i=r, \theta, \text{ or } \phi$. The analytic expressions all satisfy $\hat{\nabla}_{\mu} T_{\nu}^{\mu}=0$ on the Schwarzschild background, whose metric we denote by $\hat{g}_{\mu\nu}$.

The back reaction induced by the scalar, spinor, and vector fields is solved by calculating the fractional corrections h_{ν}^{α} in the metric,

$$g_{\mu\nu} = \hat{g}_{\alpha\mu} [\delta_{\nu}^{\alpha} + \epsilon h_{\nu}^{\alpha}], \quad (5)$$

in the semiclassical Einstein equation (1). We work in linear order in ϵ as required by $\hat{\nabla}_{\mu} T_{\nu}^{\mu}=0$ and $\hat{\nabla}_{\mu}(\delta G_{\nu}^{\mu})=0$, where δG_{ν}^{μ} is the Einstein tensor linearized on a background satisfying $\hat{G}_{\nu}^{\mu}=0$. The corrected geometry will be taken to be static and spherically symmetric. Working out the equations as in the second paper in [1], we find the corrected metric can be written as

$$ds^2 = - \left[1 - \frac{2m(r)}{r} \right] [1 + 2\epsilon\bar{p}(r)] dt^2 + \left[1 - \frac{2m(r)}{r} \right]^{-1} dr^2 + r^2 d\Omega^2, \quad (6)$$

where $d\Omega^2$ is the standard metric of a normal round unit sphere. To obtain $m(r)$ and $\bar{\rho}(r)$ requires only simple radial integrals involving T'_i and T'_r . The angular components enter linearized Einstein equations that hold automatically by virtue of $\hat{\nabla}_\mu T^\mu_\nu = 0$ in a static spherical geometry.

The mass function $m(r)$ has the form

$$m(r) = M(1 + \epsilon\mu(r) + \epsilon CK^{-1}), \quad (7)$$

with

$$\mu(r) = \frac{1}{\epsilon M} \int_{2M}^r (-T'_i) 4\pi \bar{r}^2 d\bar{r}, \quad (8)$$

and C is an integration constant which serves to renormalize the bare Schwarzschild mass M , as discussed in [1]. The metric is completed by a determination of $\bar{\rho}$ which, like μ , can be found from an elementary integration. Defining

$$K\bar{\rho} \equiv K\rho + k, \quad (9)$$

where k is a constant of integration, we have

$$\rho = \frac{1}{\epsilon} \int_{2M}^r (T'_r - T'_i)(\bar{r} - 2M)^{-1} 4\pi \bar{r}^2 d\bar{r}. \quad (10)$$

Denote with subscripts S , f , and V the metric functions and corresponding integration constants connected with the scalar, fermion, and vector back reactions, respectively. From [1] we can transcribe the relevant results. Here we give explicitly (where $w \equiv 2M/r$),

$$K\mu_S = \frac{1}{3}(1-w)(w^{-3} + 4w^{-2} + 13w^{-1} - 24w - 33w^3 - 9) - 4 \ln(w), \quad (11)$$

$$K\mu_f = \frac{1}{24}(1-w)(14w^{-3} + 56w^{-2} + 182w^{-1} - 136w - 322w^2 + 134) - 7 \ln(w), \quad (12)$$

and

$$K\mu_V = \frac{2}{3}(1-w)(w^{-3} + 4w^{-2} + 13w^{-1} - 44w - 83w^2 - 359) - 8 \ln(w). \quad (13)$$

The factor $(1-w)$ has been exhibited in each case to make clear the behavior of the proper (orthonormal frame) components h^α_ν of the perturbation near the horizon $w=1$ ($r=2M$), which we shall need later. The formulas for ρ_S , ρ_f , and ρ_V are given in suitable form in [1].

The back-reaction problem (1) has no definite solution unless boundary conditions are specified at a certain radius r_0 . Moreover, (3) indicates that the stress-energy tensors are asymptotically constant; thus the combined system of the black hole plus equilibrium quantum fields must be put into a finite "box" or cavity [1]. This is to insure that the fractional corrections ϵh^α_ν to the metric remain small for sufficiently large radius. Obviously, the box is merely a device to provide reasonable boundary conditions that mimic implantation of the hole and its equilibrating radiation into the Universe. Under suitable conditions, as discussed in [1], the specific boundary con-

ditions should not affect our results significantly. In what follows, we shall assume that the cavity radius r_0 is sufficiently large that the stress-energy tensors we employ, which were computed for infinite space, are a good approximation. If the radius r_0 were to approach the horizon, explicit size and boundary effects would have to be taken into account in the construction of $\langle T_{\mu\nu} \rangle$, as shown in [7,8].

One convenient way to fix the constant k in (9) is to impose a microcanonical boundary condition [1]. We fix r_0 and imagine placing there an ideal massless perfectly reflecting wall. Outside r_0 , we then have an ordinary asymptotically flat Schwarzschild spacetime of mass $m(r_0)$. Continuity of the three-metric across the world tube $r=r_0$ fixes the constant k , i.e., k_S , k_f , or k_V , in $\bar{\rho}$ by the relation

$$k = -K\rho(r_0). \quad (14)$$

There are finite discontinuities in the extrinsic curvature of the world tube $r=r_0$ [1], but these, and other properties of the box wall, are of no interest in the present analysis, as argued in [1].

The spacetime geometry, including back reaction, is now completely determined by a Schwarzschild metric of mass $m(r_0)$ for $r \geq r_0$, and for $r \leq r_0$ by

$$ds^2 = - \left[1 - \frac{2m(r)}{r} \right] \{ 1 + 2\epsilon[\rho(r) - \rho(r_0)] \} dt^2 + \left[1 - \frac{2m(r)}{r} \right]^{-1} dr^2 + r^2 d\Omega^2. \quad (15)$$

The parameters r_0 and ϵ must be chosen so that the corrections to the background metric remain suitably small. In other words, we must ensure that the effect of T^μ_ν is a perturbation of the Schwarzschild geometry. This requirement will be met by demanding that the proper (orthonormal frame) perturbations satisfy

$$\epsilon |h^\alpha_\nu| \equiv \delta < 1, \quad (16)$$

where the only nonzero metric perturbations are given by

$$h^r_r = w \frac{\mu(r)}{1-w}, \quad (17)$$

$$h^i_i = -2[\rho(w_0) - \rho(w)] - h^r_r, \quad (18)$$

with $w_0 \equiv 2M/r_0$. As $r \rightarrow r_0$, the first factor on the right of (18) vanishes and as r_0 becomes large, both (17) and (18) satisfy in magnitude

$$\lim_{r \rightarrow r_0, r_0 \rightarrow \infty} |h^\alpha_\nu| \sim \alpha_j (1/6K)(r/M)^2, \quad (19)$$

where $\alpha_S = \frac{1}{2}$, $\alpha_f = \frac{7}{8}$, and $\alpha_V = 1$. An asymptotic radius r_{asympt} is then roughly defined by using (19) and enforcing (16):

$$1 \leq \left[\frac{r_{\text{asympt}}}{2M} \right]^2 = \left[\frac{1}{w_{\text{asympt}}} \right] = \frac{3K}{2\alpha_j} \left[\frac{\delta}{\epsilon} \right]. \quad (20)$$

It is necessary to take $r_0 \leq r_{\text{asympt}}$. We will use $r_0 = r_{\text{asympt}}$ in the following, as well as $\delta = \epsilon$, for illustrative purposes.

It is also necessary to check $|h_v^\alpha|$ in the region $2M \leq r \leq 15M$, where most of the interesting physics occurs. The latter check is required because in most cases the maximum value of $|h_t^r|$ does not occur at the asymptotic radius. Thus, the maximum value of $|h_t^r|$ for all three spins is about two and occurs near the horizon. [There $\epsilon \leq 0.5$ is required in order to satisfy (16).] As $r \rightarrow r_{\text{asympt}} = r_0$, $|h_t^r|$ approaches one, as does $|h_r^t|$. On the other hand, h_r^t is typically small near the horizon and increases slowly to one at the asymptotic radius. It is, indeed, the behavior of h_r^t that actually determines the asymptotic radius: h_r^t is independent of the integration constant $\rho(w_0)$ that occurs in h_t^r as a result of ‘‘clock calibration’’ at $r = r_0$. An exception to the ‘‘smallness’’ of h_r^t near the horizon occurs when one has a large number (not just one, as here) of U(1) fields. This point will be discussed in Sec. V.

III. EFFECTIVE POTENTIAL

To explore the potential in the vicinity of the black hole, we can, without loss of generality, consider an equatorial slice $\theta = \pi/2$ of the corrected geometry (15). Then the four-velocity of a test particle in that background is

$$U^\mu = (i, \dot{r}, 0, \dot{\phi}), \quad (21)$$

where the overdot denotes differentiation with respect to either the proper time or an affine parameter, depending on whether the test particle is massive or massless. The square of this four-velocity is

$$g_{\mu\nu} U^\mu U^\nu = g_{tt} \dot{t}^2 + g_{rr} \dot{r}^2 + g_{\phi\phi} \dot{\phi}^2 = -\kappa, \quad (22)$$

where $\kappa = 0$ or 1, for the null and timelike cases, respectively. Because the modified spacetime geometry (15) is static and spherically symmetric, there exist two conserved quantities corresponding to the two Killing vectors $(\partial/\partial t)^\nu \equiv (1, 0, 0, 0)^\nu$ and $(\partial/\partial \phi)^\nu \equiv (0, 0, 0, 1)^\nu$ of this geometry. As for the Schwarzschild case, these constants of the motion are identified with the particle’s total energy E and orbital angular momentum (with respect to the center of symmetry) L :

$$E = -g_{\mu\nu} \left[\frac{\partial}{\partial t} \right]^\mu U^\nu = -g_{tt} \dot{t}, \quad (23)$$

$$L = g_{\mu\nu} \left[\frac{\partial}{\partial \phi} \right]^\mu U^\nu = g_{\phi\phi} \dot{\phi} = r^2 \dot{\phi}. \quad (24)$$

Combining these with (22) and using the metric components from (15) yields a first integral of the test particle’s geodesic equation:

$$[1 + 2\epsilon\bar{\rho}(r)]\dot{r}^2 + \left[1 - \frac{2m(r)}{r} \right] [1 + 2\epsilon\bar{\rho}(r)] \times \left[\kappa + \frac{L^2}{r^2} \right] = E^2. \quad (25)$$

The dependence of (25) on the boundary constant $\rho(r_0)$ is determined by the calibration of coordinate time (t) with ordinary uncorrected Schwarzschild time at $r = r_0$. Since

coordinate time has no special meaning unless the metric is asymptotically constant, we might have chosen the timelike Killing vector to be $(\partial/\partial \bar{t}) = \lambda(\partial/\partial t)$ for $\lambda = \text{const}$ instead of $(\partial/\partial t)$. This corresponds to the rescaling $E \rightarrow \bar{E} \equiv \lambda E$. Deriving the geodesic equation with this choice and taking $\lambda = [1 + \epsilon\rho(r_0)]$ yields (25) with E^2 replaced by \bar{E}^2 and $\bar{\rho}$ replaced by ρ , i.e., the integration constant $\rho(r_0)$ has been absorbed into the total energy. Note, however, that for $r \rightarrow \infty$, \bar{E} does not reduce to the special relativistic formula ($= dt/d\tau$) for the total energy (per unit rest mass) of a particle (as seen by a static observer at asymptotically flat infinity) unless $\lambda = 1$. Although it is significant that results come out without reference to a possibly nonexistent flat distant region, the direct comparison with the standard Schwarzschild case may be helpful, and we shall use E , not \bar{E} , in what follows. No actual physical observable depends on whether one uses E or \bar{E} .

For circular orbits, $\dot{r} = 0$, and the total energy E of the particle is just a function of r (velocity independent). Thus, the effective potential for a black hole modified by $O(\hbar)$ stress-energy is

$$V^2(w) = \left[\kappa + \frac{L^2}{4M^2} w^2 \right] (1-w) \times \{ 1 + \epsilon [2\bar{\rho}(w) - w(1-w)^{-1} \mu(w)] \} = \left[\kappa + \frac{L^2}{4M^2} w^2 \right] (1-w) \{ 1 + \epsilon [h_t^r(w)] \}. \quad (26)$$

Equation (25) is a differential equation for the radial coordinate. Once the radial motion is determined using this effective potential, the time coordinate change (relevant only if one refers to time at flat spatial infinity) and angular motion are easily found from (23) and (24). For $\epsilon = 0$, V^2 reduces to the effective potential of a classical Schwarzschild black hole [9]. The function defined in (26) plays the role of an effective potential, in the sense that the condition $E^2 > V^2$ determines the classically admissible range of the point particle’s motion.

A. Null orbits

Setting $\kappa = 0$ and substituting the appropriate functions μ and ρ from the solutions in [1] of the back-reaction equation into (26) yields the effective potential for null geodesics arising from scalar, fermion, or gauge boson back reactions. For simplicity and purposes of illustration, we set $\delta = \epsilon$ in (20) and find the asymptotic radii to be $r_{\text{asympt}} = 376M$, $283M$, and $265M$ for spin 0, $\frac{1}{2}$, and 1. Since the shape of V^2 is independent of the angular momentum L , we plot in Fig. 1 the functions $(4M^2/L^2)V^2$, using the appropriate functional forms for $\mu(w)$ and $\rho(w)$, to indicate the nature of the back reaction for the different spin cases and for various choices of ϵ . The $\epsilon = 0$ (i.e., no back reaction) case is displayed for reference. The effective potentials corresponding to the single-particle back reactions are qualitatively indistinguishable among the scalar, spinor, or vector cases, and Fig. 1 shows $(4M^2/L^2)V^2$ for the conformal scalar. We note for $\epsilon \lesssim 0.5$, the effective potential is qualitatively

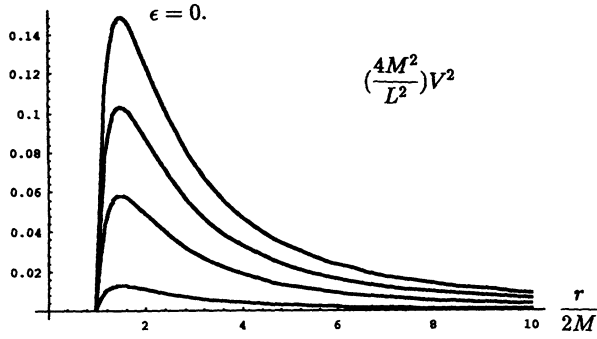


FIG. 1. Effective potential for null orbits: conformal scalar field back reaction. $\epsilon=0, 0.15, 0.3, 0.45$.

similar to the ordinary Schwarzschild case in that they exhibit maxima corresponding to a single unstable circular photon orbit, and no local minima. The location of this maximum follows from solving the equation $\partial V^2/\partial w=0$ or

$$w(2-3w) + \epsilon \left[2w(2-3w)\bar{\rho}_j - 3w^2\mu_j - \frac{32\pi M^2}{\epsilon w} (T_r^r)_j \right] = 0, \quad (27)$$

for $j=S, f$, or V . The position of the unstable circular orbit is relatively independent of variations in ϵ , and we find $\bar{r}=3.0M$ solves (27) for all spin cases to a very good approximation. What does depend strongly on ϵ is the overall magnitude of the potential. This tends to decrease as ϵ increases. Eventually, as perturbation theory becomes unreliable (for $\epsilon \gtrsim 0.5$), V^2 becomes negative and has a local minimum. This would indicate a stable circular photon orbit, but such a result cannot be established in $O(\hbar)$ for, from the form of $V^2(w)$ given in (26), it is clear that $(1+\epsilon h'_i)$ has become negative, the metric signature has changed ($g_{tt} \geq 0$), and V has become imaginary. Calculations of higher order in \hbar will be required to examine this issue further.

The lowering of the potential barrier profoundly affects the ability of the black hole to capture photons (and neutrinos, gravitons, or any massless quanta). The minimum energy E required to surmount the top of the potential barrier is given by $E(\bar{r})=V(\bar{r})$. The solutions of this equation represent the (classical) turning points of the effective potential. The apparent impact parameter of a light ray, i.e., the distance of closest approach to the black hole is $b=L/E$, and the black hole will capture any light ray sent towards it whose impact parameter is less than the critical value:

$$b_{\text{crit}} \equiv \frac{L}{E(\bar{r})}. \quad (28)$$

Thus, the photon capture cross section for the equilibrium black hole is

$$\sigma_{\text{capture}} = \pi b_{\text{crit}}^2 \geq 27\pi M^2, \quad (29)$$

and is larger than the Schwarzschild value of $27\pi M^2$ [10].

B. Timelike orbits

When $\kappa=1$ the shape of the effective potential depends on the test particle's angular momentum in an important way. Recall, for the case of the Schwarzschild black hole, V^2 will have no extrema if $L < L_{\text{crit}} = 2\sqrt{3}M$, and a particle heading towards the center of attraction will fall into the singularity no matter how far away it is initially. By contrast, when $L > L_{\text{crit}}$ the effective potential has a maximum and a local minimum, associated with unstable and stable circular massive orbits. Furthermore, when $L > 4M$, the potential will have massive bound orbits [9]. As we will see, new features show up caused by the back reaction.

Calculations of V^2 are summarized graphically in Figs. 2 and 3, where we have plotted the effective potential for various values of L and ϵ for the case of the spin- $\frac{1}{2}$ back reaction. (The other cases are qualitatively similar in every respect, and we do not include them here.) The no-back-reaction curve is included for reference. When $L < L_{\text{crit}}$, V^2 has no local extrema, as shown in Fig. 2, but the magnitude of V^2 decreases for increasing ϵ , just as for the null-orbit examples discussed above. The potential changes sign around $\epsilon \approx 0.5$. In Fig. 3 the effect of higher angular momentum is displayed, by taking $L = 2\sqrt{10}M > L_{\text{crit}}$. These curves have a local maximum (unstable circular orbit) and a local minimum (stable circular orbit). The role of these two critical points would interchange as ϵ crosses 0.5, as one goes beyond the limits of this perturbative calculation.

Unlike the null case, the impact parameter for massive particles depends on the particle's angular momentum L . The capture cross section is $\sigma_{\text{capture}} = \pi b_{\text{crit}}^2$, where the critical impact parameter is

$$b_{\text{crit}} = \frac{L_{\text{crit}}}{[E^2(r_{\text{max}}) - m^2]^{1/2}}, \quad (30)$$

and m denotes the test particle rest mass (in units where $c=1$). The energy E in (30) is the amount required to just overcome the potential barrier; i.e., $E(r_{\text{max}}) = V(r_{\text{max}})$, where r_{max} locates the maximum value of the effective potential. The value of the critical angular momentum, defined to be that value of L below

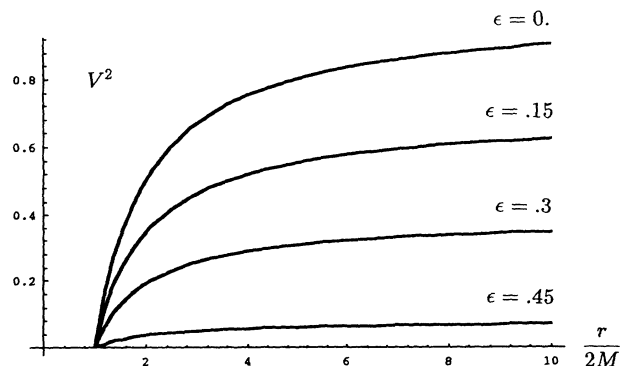


FIG. 2. Effective potential, timelike orbits for $L=0$; fermion back reaction.

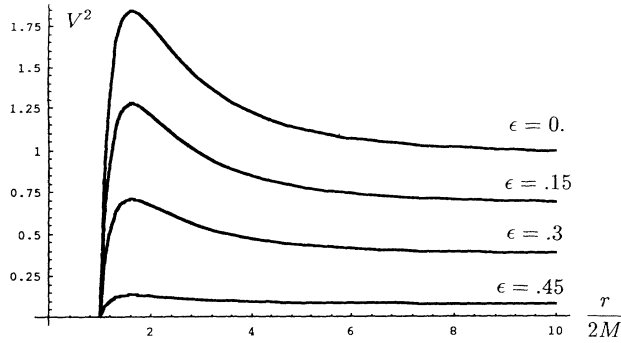


FIG. 3. Effective potential, timelike orbits for $L=2\sqrt{10}M$: fermion back reaction.

which there are no bound orbits, depends very weakly on ϵ , so that one may take $L_{\text{crit}} \approx 2\sqrt{3}M$ in (30). With the exception of the gauge boson case, the capture cross section for massive test particles tends to increase with the strength of the back reaction. This is caused by the lowering of the potential barrier at $r=r_{\text{max}}$.

IV. REPULSIVE GRAVITY

Additional physical insight into the consequences of the back reaction is provided by a study of the acceleration of a test particle in the modified spacetime geometry (15). The acceleration gives a direct probe of the force acting on the particle.

Here, we consider a massive test particle initially at rest; this is equivalent to setting $L=0$ in the timelike ($\kappa=1$) effective potential (26). The four-velocity of a particle at rest is

$$U^\mu = \left(\frac{dt}{d\tau}, 0, 0, 0 \right), \quad (31)$$

where τ is the proper time, and its acceleration is

$$a^\mu = \frac{dU^\mu}{d\tau} + \Gamma_{\alpha\beta}^\mu U^\alpha U^\beta. \quad (32)$$

From (22) and (31), with $\kappa=1$ we have $(dt/d\tau)^2 = (-g_{tt})^{-1}$, so the radial component of the acceleration is

$$a^r = \left(\frac{dt}{d\tau} \right)^2 \Gamma_{tt}^r = \frac{1}{2} g^{rr} \frac{\partial}{\partial r} \ln(-g_{tt}). \quad (33)$$

Transforming to the particle's proper rest frame (local orthonormal frame) gives

$$a^{\hat{r}} = \frac{1}{2} (g^{rr})^{1/2} \frac{\partial}{\partial r} \ln(-g_{tt}), \quad (34)$$

where the caret refers to components with respect to this frame; i.e., $g_{\hat{\mu}\hat{\nu}} = \text{diag}(-1, 1, 1, 1)_{\hat{\mu}\hat{\nu}}$.

Evaluation of $a^{\hat{r}}$ requires knowledge of the metric components g^{rr} and g_{tt} to $O(\epsilon)$. These can be read off from (15), and when written in terms of w are

$$g^{rr} = (1-w)[1 - \epsilon(1-w)^{-1}w\mu(w)], \quad (35)$$

and

$$-g_{tt} = (1-w)\{1 + \epsilon[2\bar{\rho}(w) - w(1-w)^{-1}\mu(w)]\}. \quad (36)$$

After some algebra, using (8) and (10) to calculate $\partial\mu/\partial w$ and $\partial\rho/\partial w$, we arrive at the compact expression

$$a^{\hat{r}} = (1-w)^{-1/2} \left[\frac{w^2}{4M} \right] [1 + \epsilon\Delta^{\hat{r}}], \quad (37)$$

for the radial acceleration of a particle at rest, where

$$\Delta^{\hat{r}} \equiv (1-w)^{-1} \left[1 - \frac{w}{2} \right] \mu(w) + \frac{32\pi M^2}{\epsilon w^3} T_r^r, \quad (38)$$

is the correction caused by the back reaction. $\Delta^{\hat{r}}$ is independent of ϵ : indeed, the “ ϵ pole” in the second term is exactly canceled by the coefficient (4) which multiplies all the expressions for the stress-energy tensors.

It is a straightforward exercise to compute $\Delta^{\hat{r}}$ for the scalar, spin- $\frac{1}{2}$, and vector boson back reactions by substituting the corresponding μ_j and $(T_r^r)_j$ into (38) for $j=S, f$, and V . We find that both

$$\Delta_S^{\hat{r}} > 0 \text{ and } \Delta_f^{\hat{r}} > 0, \quad \forall r \geq 2M, \quad (39)$$

but

$$\Delta_V^{\hat{r}} < 0, \quad (40)$$

for $2.8M \lesssim r \lesssim 8.6M$. In other words, while the conformal scalar and massless spinor back reactions appear to make the “dressed” black hole more attractive (we have seen this effect from the effective potential point of view, in the lowering of the magnitude of the effective potential for timelike orbits; see Figs. 2 and 3), the gauge boson back reaction tends to weaken the attractive force of the black hole by generating a localizing spherical region or “shell” containing a repulsive component of the net force. Since we have set $L=0$ from the outset, this cannot be an artifact of the particle's orbital motion (it is stationary), but must be ascribed to a genuine repulsive gravitational force, or *antigravity*, completely quantum mechanical in origin and induced by the U(1) back reaction.

V. MULTIPLE FIELD BACK REACTION

Thus far we have investigated the separate back reactions due to single species, either a conformal scalar, a massless spinor, or a U(1) gauge field. While this has revealed novel important features of the back-reaction problem, a more realistic setting should take into account black holes in thermal equilibrium with a heat bath comprising multiple species of quantum fields. We know from elementary particle physics that the replication or multiplicity of scalars, fermions, and gauge fields reflects the variety of quantum numbers needed to distinguish physical attributes (flavor, color, mass, etc.) observed directly or inferred from observation. Particle replication is also the starting point for constructing unified models of the fundamental interactions based on large (i.e., rank 4 or greater) gauge groups [11].

Apart from the details of their specific phenomenologies, what primarily distinguishes say, the standard model (SM) from one or more of the grand unified theories (in

which the SM must be embedded) is the particle content and group-theoretic assignment of each model. This is determined once the choice of gauge group is made and the scalars (Higgs bosons) and fermions (quarks and leptons) have been assigned to various multiplets or representations of the group. These group theory assignments can be characterized with a set of integers. The number N_V of gauge bosons belonging to a given gauge group is given by the number of group generators. (See the last reference in [1] and also [2].) Typically, the number of fermions (N_f) is the dimension of the representation times the number of families, and the number of scalars (N_S) is determined by the pattern of symmetry breaking to smaller groups one wishes to explore. We shall give examples of the N_j below for the standard model as well as for some generic extensions of this model.

In the limit of free field theories on a background spacetime, the back reaction due to a collection of fields is easy to treat. This follows because the stress-energy tensors in this limit only depend quadratically on the fields and are “flavor diagonal.” To make this point clear, we note the stress-energy tensor for a set of N_S real massless conformally coupled scalars is

$$\mathcal{T}_\nu^\mu = \sum_{k=1}^{N_S} (T_\nu^\mu)^k, \quad (41)$$

where (no sum on k)

$$(T_{\mu\nu})^k = \frac{2}{3} \Phi_{,\mu}^k \Phi_{,\nu}^k - \frac{1}{6} g_{\mu\nu} g^{\sigma\rho} \Phi_{,\sigma}^k \Phi_{,\rho}^k - \frac{1}{3} \Phi^k \Phi_{,\mu\nu}^k - \frac{1}{12} g_{\mu\nu} \Phi^k \square \Phi^k, \quad (42)$$

is the tensor for a single scalar. Then, upon renormalization,

$$\langle \mathcal{T}_\nu^\mu \rangle_{\text{ren}} = \sum_{k=1}^{N_S} \langle (T_\nu^\mu)^k \rangle_{\text{ren}} = N_S \langle T_\nu^\mu \rangle_{\text{ren}}, \quad (43)$$

where the last equality follows from the fact that the renormalization procedure is independent of the species label k . Similar considerations hold for the renormalization of the spin- $\frac{1}{2}$ and gauge boson tensors in the multiple particle case [12].

The upshot of this is that we should obtain a good approximation to the multiple field (and multiple spin) back reaction in the limit of small gauge, Yukawa, and scalar self-couplings by simply replacing the source term in (1) by an appropriate weighted combination (with weights N_S , N_f , and N_V) of the single-species stress-energy tensors. From (1), (8), and (10), this entails the rescaling

$$\mu(r)_j \rightarrow N_j \mu(r)_j, \quad \text{and} \quad \rho(r)_j \rightarrow N_j \rho(r)_j, \quad (44)$$

for $j=S, f, V$. To get a feeling for the values of the

“weights” one can expect, we give a brief listing of the numbers of gauge fields, spinors, and real scalars contained in typical gauge theories in Table I. The standard model of elementary particles contains a total of 12 gauge bosons (8 gluons, the W^+ , W^- , Z^0 , and the photon), requires at least one complex scalar doublet (4 real scalars) for spontaneous symmetry breaking, and has three families of 15 quarks and leptons (45 spinors) [13]. The Bose-Fermi symmetry of supersymmetry doubles the particle spectrum of the nonsupersymmetric models. For the minimal supersymmetric standard model (MSSM), there are the 12 gauge bosons, the spin- $\frac{1}{2}$ sector is augmented over that of the SM by the addition of 12 gauginos (fermionic partners of the gauge bosons) and from the fermionic partners of the two complex scalar doublets (8 real scalars) needed to break the gauge symmetry and provide fermion masses in this model [11]. This yields a total $N_f=65$. The 45 original fermions of the SM have 45 spin-0 partners which add to the two complex doublets to give a total $N_S=53$. The smallest simple group containing the SM is SU(5). This has 24 gauge fields, 45 quarks and leptons (3 families of 15), and scalars in the adjoint 24, and a fundamental 5 complex representation, or 34 real scalars in total [11]. Finally, Table I includes an E_6 model which contains 78 gauge particles, three families of 27 fermions, and an adjoint 78 (real) and two 27’s of (complex) scalars.

An important consequence of the multiple-field back reaction is that the permissible asymptotic radius is smaller, for a given $\epsilon > 0$, than for the $N=1$ cases. This can be appreciated immediately by inspection of (17) and (18), which show that the metric perturbations grow in direct proportion to the N_j . This growth shrinks the asymptotic radius according to

$$1 \leq \left[\frac{r_{\text{asympt}}}{2M} \right]^2 = \frac{3K}{2\alpha_j N_j} \left[\frac{\delta}{\epsilon} \right]. \quad (45)$$

Nevertheless, because K is such a large constant, we can still find perturbatively valid solutions of (1) involving large numbers of conformal scalar and fermion fields. The case of gauge bosons is more interesting. Here we find, unlike the other spins, a basic limitation on N_V arising from the magnitude of h_r^i at the horizon. This is independent of the choice of asymptotic radius. We find

$$(h_r^i)_V|_{r=2M} = -0.0252, \quad (46)$$

which implies that $N_V \epsilon < 38$ is required. With $\delta = \epsilon$, an examination of h_r^i shows that we can choose, for example, $r_{\text{asympt}} = 27M$. In Fig. 4, we plot the null potential for $N_V = 84$ and $\epsilon = 0, 0.15$, and 0.45 . It appears that there is a tendency towards the formation of a stable circular or-

TABLE I. Particle multiplicities of various gauge theories.

Model	Gauge group	N_V	N_f	N_S
Standard model (SM)	SU(3)⊗SU(2)⊗U(1)	12	45	4
Minimal SUSY SM	SU(3)⊗SU(2)⊗U(1)	12	65	53
Minimal SU(5)	SU(5)	24	45	34
Three family E_6	E_6	78	81	186

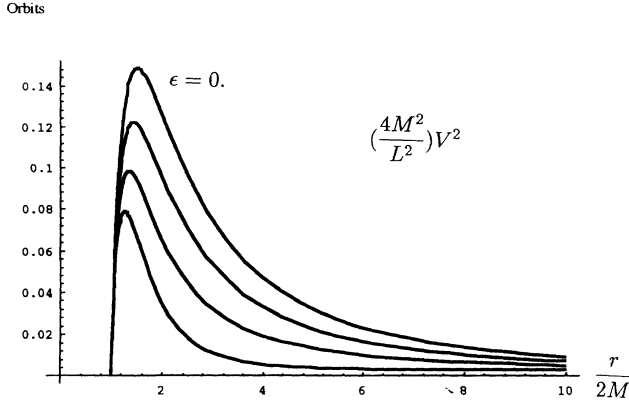


FIG. 4. Effective potential, null orbits: gauge field back reaction with $N_V = 84$. $\epsilon = 0, 0.15, 0.30$, and 0.45 .

bit with $V^2 > 0$, but we cannot establish this unambiguously.

In spite of the limitations imposed by the perturbative constraints, it is tempting to try to discover what *might* emerge in a full-fledged (i.e., numerical or nonperturbative) calculation. To this end, we consider the examples displayed in Figs. 5 and 6 where we have set the gauge boson multiplicity $N_V = 300$ ($r_{\text{asympt}} = 15M$). We point out that, for example, the string-inspired unification group $E_8 \otimes E_8$ contains 496 gauge bosons, so a multiplicity on the order of 300 is not unrealistic. Here, as the back reaction is increased, the barrier peak associated with the null potential (Fig. 5) *increases* while the rest of the potential flattens out. This phenomena shows up only for the gauge field case, and is due to the amplification of the repulsive region which, as we have noted, exists only for this case. Note the no-back-reaction curve ($\epsilon = 0$) has the lowest barrier of the set of potential curves. Similar amplification might take place for the timelike effective potential, as indicated in Fig. 6. Again, for illustrative purposes only, we take $N_V = 300$, the same range of ϵ as before, but with $L = 0$. Without the back reaction, the test particle would be doomed to be captured by the black hole, as is well known. However, in the present case, this extrapolation to very large gauge boson multiplicities may prevent the test particle from being captured, even for vanishing impact parameter.

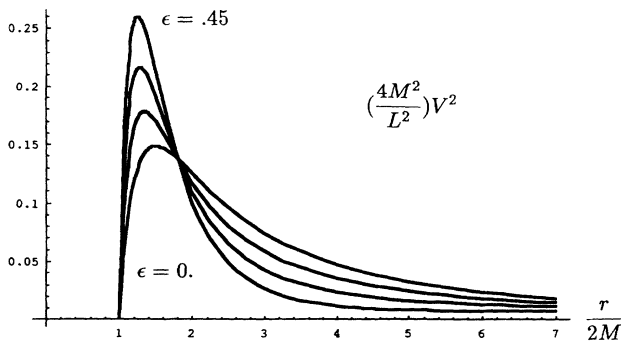


FIG. 5. Effective potential, null orbits: gauge field back reactions with $n_V = 300$.

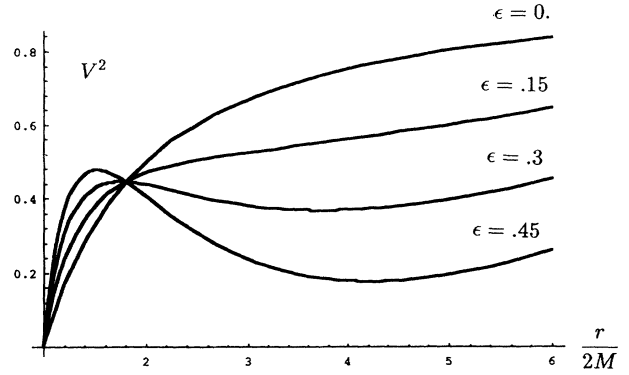


FIG. 6. Effective potential, timelike orbits for $L = 0$: gauge field back reaction with $N_V = 300$.

VI. DISCUSSION

The lowest order solutions of the back-reaction problem solved in this paper contain rather striking features that are revealed through calculations of the black hole effective potential. We have found the back reaction tends to diminish the overall magnitude of the potentials corresponding to null and timelike orbits. This lowering of the effective potential is correlated with an associated increase in the black hole capture cross sections for those instances when the potential exhibits a barrier peak. This, in turn, can be expected to affect the black hole lifetime which results from the competition between particle capture and evaporation if the hole is formed in thermal equilibrium and subsequently goes out of equilibrium with the surrounding particle heat bath [10]. For “extreme” values of the perturbation parameter ($\epsilon \gtrsim 0.5$) the potentials turn over completely, become negative near the renormalized event horizon, and exhibit minima corresponding to bound orbits. Although an ϵ approaching such values is surely pushing the limits of perturbation theory, perhaps beyond the bounds of even qualitative reliability, nevertheless, one may interpret these results as indicating possible qualitative trends which should be investigated in more nearly complete treatments.

The shapes and magnitudes of the effective potentials are similar for the single-species back reactions from the spin-0, $-\frac{1}{2}$, and -1 fields, but the U(1) case merits special attention. The gauge boson back reaction generates a repulsive force in the neighborhood of the event horizon, which is revealed by calculating the radial acceleration of a massive test particle placed initially at rest outside the black hole. The component of the net force due to the back reaction points away from the origin, unlike the scalar and fermion cases, where it points inward. The appearance of such Casimir-type forces, which are quantum-mechanical in origin, should be expected on general grounds. Indeed, as emphasized in [14], a meaningful definition of the physical vacuum energy must take into account the fact that quantum fields always exist in the presence of external constraints, i.e., either in interaction with matter or other external fields or boundaries. For the cases at hand, the renormalization of the stress-energy tensors employed here must take into account

that the quantum fields (the scalar, spinor, and gauge boson) interact with the classical background Schwarzschild spacetime. This external "constraint" affects the zero-point modes of the quantum fields which in turn affects the zero-point energies.

The treatment of multiple-species back reaction is useful for problems involving black holes in thermal equilibrium with heat baths made up from fields belonging to representations of gauge theories. Again, the gauge-boson example is particularly noteworthy since an increase in the number of gauge fields can substantially amplify the repulsive gravitational Casimir force. Since all spins discussed in this paper come into play for the back reaction due to a gauge theory with matter, it may prove worthwhile to study the cosmology of models that lead to a net increase or decrease in the capture cross section [10].

Provided the semiclassical back-reaction program leads qualitatively in the right direction (that is, towards a correct quantum gravity), one should include the spin-2

graviton contribution to the renormalized one-loop effective stress-energy tensor. The effects of linear gravitons should contribute a term to the stress-energy tensor of the same order as those coming from ordinary matter and radiation fields.

Finally, not all scalars will be conformally coupled to the curvature nor will they necessarily be massless. For example, the Higgs scalars could couple with any strength to the curvature. Partial results from a calculation of the renormalized stress-energy tensor of a scalar with arbitrary coupling and mass has recently been published and could serve as a starting point for a more general investigation of the scalar field back reaction [15].

ACKNOWLEDGMENTS

This research was supported by DOE Grant No. DE-FG05-85ER40226 (D.H. and T.W.K.) and by National Science Foundation Grant PHY-8908741 (J.W.Y.).

-
- [1] D. Hochberg, T. W. Kephart, and J. W. York, *Phys. Rev. D* **48**, 479 (1993); J. W. York, *ibid.* **31**, 775 (1985); D. Hochberg and T. W. Kephart, *ibid.* **47**, 1465 (1993).
- [2] M. A. Abramowicz and A. R. Prasanna, *Mon. Not. R. Astron. Soc.* **245**, 720 (1990); M. A. Abramowicz and J. C. Miller, *ibid.* **245**, 729 (1990); M. A. Abramowicz, *ibid.* **245**, 733 (1990).
- [3] K. W. Howard, *Phys. Rev. D* **30**, 2532 (1984); K. W. Howard and P. Candelas, *Phys. Rev. Lett.* **53**, 403 (1984).
- [4] B. P. Jensen and A. Ottewill, *Phys. Rev. D* **39**, 1130 (1989).
- [5] D. N. Page, *Phys. Rev. D* **25**, 1499 (1982).
- [6] M. R. Brown, A. C. Ottewill, and D. N. Page, *Phys. Rev. D* **33**, 2840 (1986).
- [7] T. Elster, *J. Phys. A* **16**, 989 (1983).
- [8] T. Elster, *Class. Quantum Grav.* **1**, 43 (1984).
- [9] C. W. Misner, K. S. Thorne, and J. A. Wheeler, *Gravitation* (Freeman, San Francisco, 1973). The effective potential is discussed in Chap. 25.
- [10] These results will be discussed in a forthcoming paper in progress.
- [11] G. G. Ross, *Grand Unified Theories* (Benjamin-Cummings, Menlo Park, CA, 1984).
- [12] In the Abelian limit, the relation between renormalized stress-energy tensors for gauge groups G and $U(1)$ is $\langle T_{\mu\nu} \rangle_G = N_V \langle T_{\mu\nu} \rangle_{U(1)}$. N_V is given by the number of group generators in G . In the last reference in [1], the second Casimir invariant $C_2(G)$ should be replaced everywhere by N_V .
- [13] Chris Quigg, *Gauge Theories of the Strong, Weak, and Electromagnetic Interactions* (Benjamin-Cummings, Menlo Park, CA, 1983).
- [14] G. Plunien, B. Müller, and W. Greiner, *Phys. Rep.* **134**, 87 (1986).
- [15] P. Anderson, W. Hiscock, and D. A. Samuel, *Phys. Rev. Lett.* **70**, 1739 (1993).